INTERNATIONAL JOURNAL OF INTEGRATED ENGINEERING
ISSN: 2229-838X e-ISSN: 2600-7916

IJIE

Vol. 16 No. 1 (2024) 201-212
https://publisher.uthm.edu.my/ojs/index.php/ijie

Shear Strength of Adhesively Bonded Joint with Toughened Epoxy Mussel Powder

Subashini Velayutham[1], Sugiman Sugiman[2], Hilton Ahmad[1]*, Zainorizuan Mohd Jaini[1]

[1] *Faculty of Civil Engineering and Build Environment, Universiti Tun Hussein Onn Malaysia, 86400 Parit Raja, Johor, MALAYSIA*
[2] *Faculty of Engineering, University of Mataram, Mataram, West Nusa Tenggara, 83115, INDONESIA*

*Corresponding Author: hilton@uthm.edu.my
DOI: https://doi.org/10.30880/ijie.2024.16.01.016

Article Info

Received: 14 September 2023
Accepted: 18 March 2024
Available online: 22 May 2024

Keywords

Mussel shell, filler, toughened epoxy resin, single lap joint, shear strength

Abstract

Synthetic fillers were usually used to improve the shear strength of epoxy resin, but dependency on mineral-derived substances may increase the greenhouse effect. To surmount the problem, biofiller from household wastes mussel shells is proposed to improve the mechanical properties of epoxy due to its high calcium carbonate content. In this paper, the physical properties (X-ray diffraction test) and shear strength of toughened epoxy with mussel shell powder (TEMP) were investigated. Single lap joints (SLJ) specimens were tested for shear strength with incorporation of various TEMP volume fractions and over-lap length. The testing series includes TEMP volume fractions from 0% to 10% (by 2.5% increment) and overlap length ranging from 12.7 to 50.8 mm. The results demonstrated that the longest overlap length and 7.5% TEMP volume fractions exhibited a significant effect on the ultimate joint strength. From scanning electron microscopy (SEM), 10% TEMP was prone to particle agglomerations and gave less joint strength. The joint strength with 7.5% mussel shell powder was stronger compared with other volume fractions, with strength enhancement from 103.7% to 169.6% for the studied overlap lengths.

1. Introduction

According to Lu et al. [1], neat epoxy resin is a typical cross-linked thermosetting polymer material with several benefits, including exceptional mechanical qualities, high stability and bonding ability, minimal shrinkage, and excellent chemical resistance. Epoxy adhesives are widely used to join metal-metal, metal-composite, and composite-composite in industrial sectors such as automobile, electronics, and civil engineering sectors. However, epoxy resin has low shear strength, which limits its applicability to structure applications. Rigid particles can be added to the epoxy as filler to improve its shear strength and associated mechanical properties such as elastic modulus and tensile strength. Formerly, micro-silica and zirconia fillers were added in neat epoxy resin. However, these synthetic materials are derived from minerals that may contribute to the green-house effect. In more recent years, due to environmental awareness, researchers have shifted to using waste material, such as fly ash [2]. However, fly ash has been commercialized (to produce blended cement), and many countries have started to implement renewable energy; therefore, the availability of this coal-combustion by-product is limited. Due to the presence of calcite, eggshells and mussels started to get attention and were used as fillers in neat epoxy resin [3]. The smaller micron-size particles may promote higher surface area and offer better mechanical properties when

mixed with epoxy resin, but too small particles are prone to agglomerate as it is sensitive to the presence of moisture.

Mechanically fastened joints, adhesive joints, or hybrid joints can be used to join two parts of structures. The former joining types are usually adopted but have the drawbacks of stress concentration, weight penalty and the ability to combine different materials [4]. An adhesively bonded joint is a method of assembling two parts together, often joined by using polymeric adhesive material. The polymeric materials used were epoxy, vinyl ester, and polyester, which require proper curing of sufficient heat, time, and pressure. The load transmission in an adhesively-bonded joint is shear and bearing stress. However, the distributions of shear and peel stresses along the adhesive bond line are unbalanced, as the end of joints experience the highest peel stress, while the central regions are less affected [5]. Adhesively bonded connections provide several advantages over traditional joints such as welded, bolted, or riveted, including lower weight, more uniform stress distribution and lack of damage in the bonded components.

Single-lap adhesive joints (SLJ) were studied in most literature [6], [7] and used in actual practice due to simplicity and efficiency. Single lap joints are commonly used in the aerospace and automotive industries because the adherend thickness is comparatively thin [8]. One of the main areas of investigation in the field of adhesive bonding is to develop ways of reducing these stress concentrations for a more efficient adhesive joint strength and additional weight savings. Furthermore, the offset between the adherends generates a secondary bending moment, resulting in peel stresses along the bond line's edge. Numerous techniques to increase joint strength were proposed, but mostly showed uneven stress distribution within the adhesive [9]. The joint strength of SLJs can be increased by investigating optimum joint geometry, introducing fillet at the adhesive edge, and shape of the spew fillet.

In a different investigation, Gigante et al. [10] used mussel shell powder as reinforcement for polylactic acid (PLA), which is more suitable for thermoplastic materials that are processed below 400°C. Its low concentration of large particles achieved a different distribution from the commercial $CaCO_3$ and exhibited an average weight aspect ratio of 2.6. The bio-composite with 10%wt mussel shell achieved the most optimum result with 2.35 GPa elastic modulus, 38 MPa maximum stress, 5 kJ/m^2 Charpy impact strength, and elongation at break over 100%. The excessive hard fillers exhibited stress concentration and barrier to crack growth. Calcium carbonate in brittle matrix improves the fracture toughness during debonding mechanisms.

In the previous study, Delzendehrooy et al. [11] investigated the strength improvement of adhesively bonded single lap joints with date palm fibers considering the effect of type, size, treatment method and density of fibers. The author introduced fibers of various diameters (0.5-2 mm) into the epoxy adhesive. Three distinct weight ratios of date palm fibers (2, 5, and 10 wt%) were experimentally examined in order to determine the ideal weight ratio of the fibers correlating to maximum joint strength. The findings demonstrate that date palm fibers greatly increase the adhesively attached joints' strength. There was a 140% improvement in the strength of adhesive single-lap joints reinforced with 2 wt% Rachis fiber treated with 6% NaOH solution. The broken surfaces were examined in order to look into the micromechanisms behind failure. Anac and Dogan [12] reported the organic shells (olive pomace and walnut powders) to fill the epoxy adhesive with the content of 5, 15 and 30wt% and were used to bond the steel adherend. They found that the single lap joint strength was improved by adding 5wt% of those organic powders and the walnut powder has the better strength than that of oil pomace. Yip et al. [13] investigated the effect of volume fraction of eggshell toughened epoxy adhesive on the strength of kenaf fiber reinforced polymer and steel joints and found that the egghells volume fraction of 5% gave the optimum strength.

As environmental pollution becomes a crucial issue, engineers' essential aim is to use biodegradable materials that help reduce pollution. Therefore, bio-degradable materials or recyclable waste are becoming fillers in epoxy resin system. The addition of fillers into the epoxy resin has been proven to increase the epoxy's mechanical performance, such as wear, strength, improved machinability, and thermal properties. Among the available bio-waste additives, the widely accessible and inexpensive mussel shells contain a high amount of calcium carbonate ($CaCO_3$). The crystal structure of mussel shell generates large amounts of calcite and aragonite, which can enhance the strength of epoxy. To best authours knowledge, the appkication of mussel shell poder as filler of epoxy adhesive to bond steel substrate is rarely reported. Therefore, this study aims to analyse and evaluate the effect of mussel shell powder volume fraction on the static shear strength of SLJ compared to a neat-epoxy system.

2. Experimental Works

This section describes the experimental works investigating the effectiveness of using mussel shell powder as a filler by concentrating on TEMP volume fraction in adhesively bonded joints.

2.1 Testing Series

Each testing series was prepared with three testing specimens. Each testing series was labelled with testing designations comprised of three letters to denote joint types, TEMP volume fraction and overlap length. Table 1 shows the testing series investigated in this research framework. A combination of four different overlap lengths

Int. Journal of Integrated Engineering Vol. 16 No. 1 (2024) p. 201-212

of test specimens ranges from 12.7 mm (0.5 inch), 25.4 mm (1 inch), 38.1 mm (1.5 inch), and 50.8 mm (2 inch) and four volume fractions of mussel shell powder 0%, 2.5%, 5.0%, 7.5% and 10.0% to give a total of twenty testing series were investigated. A total of sixty testing specimens, replications of three specimens, were prepared for each testing series to obtain an average ultimate load at failure.

Table 1 *Testing series investigated*

Volume fraction of mussel powder (%)	Overlap length (mm)	Testing designations
0	12.7	SLJ-0-12.7
	25.4	SLJ-0-25.4
	38.1	SLJ-0-38.1
	50.8	SLJ-0-50.8
2.5	12.7	SLJ-2.5-12.7
	25.4	SLJ-2.5-25.4
	38.1	SLJ-2.5-38.1
	50.8	SLJ-2.5-50.8
5.0	12.7	SLJ-5-12.7
	25.4	SLJ-5-25.4
	38.1	SLJ-5-38.1
	50.8	SLJ-5-50.8
7.5	12.7	SLJ-7.5-12.7
	25.4	SLJ-7.5-25.4
	38.1	SLJ-7.5-38.1
	50.8	SLJ-7.5-50.8
10.0	12.7	SLJ-10-12.7
	25.4	SLJ-10-25.4
	38.1	SLJ-10-38.1
	50.8	SLJ-10-50.8

2.2 Preparation of Mussel Shell Powder

The mussel shells were collected from food traders within Parit Raja, Johor, Malaysia. They were then cleaned to remove the intact membrane and protein trace. The sample was immersed in sodium hydroxide (NaOH) solution to remove the stratum corneum, as shown in Fig. 1. Then, the mussel shells were dried under direct sunshine for three days. The dried mussel shells were crushed into smaller shell pieces with a mortar pounder and oven-dried at 120°C for 24 hours. Later, the mussel shells were crushed using Aggregate Impact Value (AIV) and ground using a blender to obtain sufficient powder fineness. Then, the ground mussel shell powder was sieved to pass 75 µm size using a sieving machine. The sieved mussel shell powder was later heated at 100°C for three hours to eliminate moisture. To avoid direct interaction with the atmosphere, the mussel powder was transferred into an airtight container and used to produce TEMP within three days of sieving.

(a) **(b)**

Fig. 1 (a) *Mussel shell; (b) Mussel powder*

2.3 Surface Preparation of Joining Adherends

The adherends were made of low carbon steel (also known as mild steel) Grade C15, with a carbon content of 0.15%. The elastic modulus, tensile strength and Poisson ratio of adherend are 210 GPa, 570 MPa and 0.28, respectively. It has a low carbon percentage, often ranging from 0.05% to 0.3%, which makes it more malleable and ductile than other steel varieties. Furthermore, it is softer and has lower yield strength and low cost. According to Baldan [14], the adherend surfaces determined the quality of an adhesive bond and joint strength. Surface treatments are highly recommended prior to applying adhesives to ensure excellent bond strength. Initially, the surfaces were cleaned using acetone. Next, fine-grit sandpaper was used to remove surface deposits by lightly abrading the surface of steel plates and soaked with acetone solution to eliminate impurities of the adherend surfaces. The steel plates were then heated to 120°C in the oven prior to the application of adhesive bonding. Moreover, the most typical misperception about surface preparation is that a clean surface is essential for a strong adhesive.

2.4 Preparation of Toughened Epoxy with Mussel Powder (TEMP)

A mixture of Epikote Resin 828 and Hardener 651 are used as matrix binder systems. Epikote 828 is a medium viscosity liquid epoxy resin produced from Bisphenol A resin and epichlorohydrin. EPIKOTE 828 provides good pigment wetting, resistance to filler settling, and a high level of mechanical and chemical resistance properties in the cured state. Hardener 651 is a curing agent that chemically reacts with the resin-reactive sites to create a cured polymer.

Mussel shell powder with a volume fraction, V_f of 0, 2.5, 5.0, 7.5 and 10% were prepared separately to mix with a matrix binder system with resin to hardener mixing ratio of 5:2 (by volume), as recommended by the manufacturer. The mixture was stirred gently for about 5 minutes at room temperature using a magnetic stirrer to achieve a homogeneous and uniform mixture. Poor adhesive performance might be due to a flaw mixing technique that entrapped voids. According to Loeffen et al. [15], the epoxy resin mixture must be degassed for at least 10 minutes under a vacuum chamber to remove the entrapped air inside the mussel shell pores. The degassing process is shown in Fig. 2 to allow entrapped air bubbles to be removed from the epoxy system. After that, the mixture was used immediately as adhesive material for bonding to avoid creating excessive air bubbles and allowed to cure for at least 24 hours at room temperature.

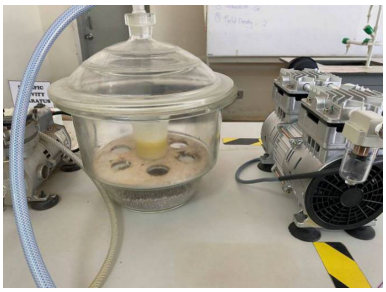

Fig. 2 *Degassing process of TEMP*

2.5 X-Ray Diffraction Analysis (XRD)

Copper K-α radiation of 0.15406nm was used to evaluate raw mussel shell powder samples for X-ray diffraction studies at voltages of 30 kV, currents of 16 mA, scan ranges of 10-90 θ, and scan rates of 8.0/min as shown in Fig. 3(a). X-ray diffraction analysis (XRD) is a non-destructive technique that provides physical properties, crystallographic structure, and chemical composition of the mussel shell powder used. The ground mussel shell powder was sieved with a sieve size of 65 µm using a sieving machine. X-ray diffraction (XRD) analysis is an analytical technique that involves shining X-rays onto a sample and measuring the diffraction pattern produced by the X-rays. This diffraction pattern contains information about the structure, phase composition, and other structural properties of the mussel shell powder being analyzed.

2.6 Morphology of the Fracture Specimen

CIQTEK SEM5000 was used to evaluate raw mussel shell powder samples for scanning electron microscope studies at voltages of 20 kV as shown in Fig. 3(b). Scanning electron microscope (SEM) uses a focused beam of high-energy electrons to produce a range of signals at the surface of solid objects. The signals are generated by electron-sample interactions to provide external appearance (texture), chemical content, crystalline structure, and orientation of the constituent parts. A scanning electron microscope (SEM) was used to do a microscopic analysis of the dog bone sample of TEMP to determine how it influences joint strength and fracture energy values.

Int. Journal of Integrated Engineering Vol. 16 No. 1 (2024) p. 201-212

The surfaces of samples were coated with gold before being inspected under the microscope to make them more conductive and improve picture quality before the SEM test. Moreover, spurred gold-plating serves as a shield to prevent specimen damage caused by excessive voltage during testing. The morphology of the shattered surfaces of the TEMP dog bone specimens was then directly examined on the gold-plated specimens. The ground contact between the specimen surface and the SEM sample holder is a copper tape made of soil copper foil. It retains the specimen position straight and offers superior conductivity for SEM testing. Images of the shattered specimens were taken and transferred to a linked computer using the appropriate magnifications.

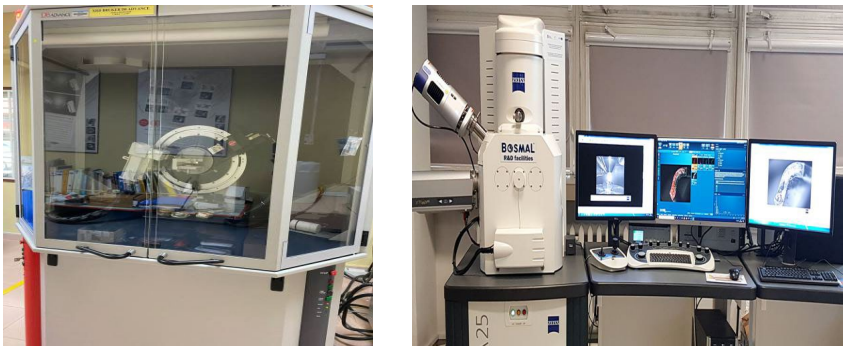

(a) **(b)**

Fig. 3 *(a) XRD test; (b) SEM test*

2.7 Fabrication of Adhesively-Bonded Single Lap Joint and Testing

A single-lap joint is created by adhering two overlapping surfaces together using epoxy resin, which often results in an adhesively bonded joint [16]. The single lap joint test specimen was fabricated according to the ASTM D1002. After the adherends were surface treated as discussed in the sub-Section, the adherends were ready to be bonded. The mussel powder-toughened epoxy adhesive, which was prepared before (see Subsection 2.3), was applied evenly over the intended overlap zone. The adhesive bonding thickness was controlled using a catgut thread with a 0.2 mm diameter. The bonding of the connecting adherends was sealed with a clip. Good interfacial contact between the adhesive-adherends layer was achieved by allowing the applied adhesive to cure at room temperature for 24 hours prior to the mechanical testing. The dimensional detail of the SLJ is shown in Fig. 4.

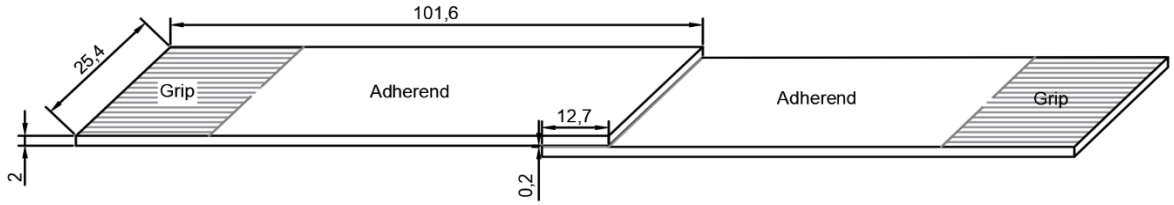

Fig. 4 *SLJ assembly and dimensions. All units in mm*

An INSTRON universal testing machine was used for mechanical testing. The test was conducted at a displacement rate of 0.5 mm/min until fracture. During testing, two steel spacers were attached at the end-tab for gripping to eliminate primary bending as shown in Fig. 5(b). Three specimens were prepared for reproducibility for each testing series.

(a) **(b)**

Fig. 5 *(a) SLJ specimens ready for mechanical testing; (b) mechanical testing using UTM machine*

3. Results and Discussion

This section presents the experimental observations and discusses the results obtained from all tested series investigated.

3.1 X-ray diffraction (XRD)

An X-ray diffraction spectrum of powdered raw mussel shell is shown in Fig. 6. The X-ray diffractogram of the powdered mussel shell showed consistent peaks that exactly matched with Aragonite $CaCO_3$ concentrations. The aragonite peaks were indicated by blue triangular markers on the corresponding peaks. Furthermore, there are several peaks at 2θ, which are 26.5, 27.5, 31.0, 36.1, 37.1, 38.0, 41.1, 43.0, 46.0, 48.5, 50.1, 52.5, 53.0, 66.0, and 69.0 respectively. Besides, the highest peak intensity was observed at 26.5°. A similar finding was reported by Macha et al. [17], where an X-ray diffractogram of the raw mussel mytilus showed consistent peaks matching calcium carbonates.

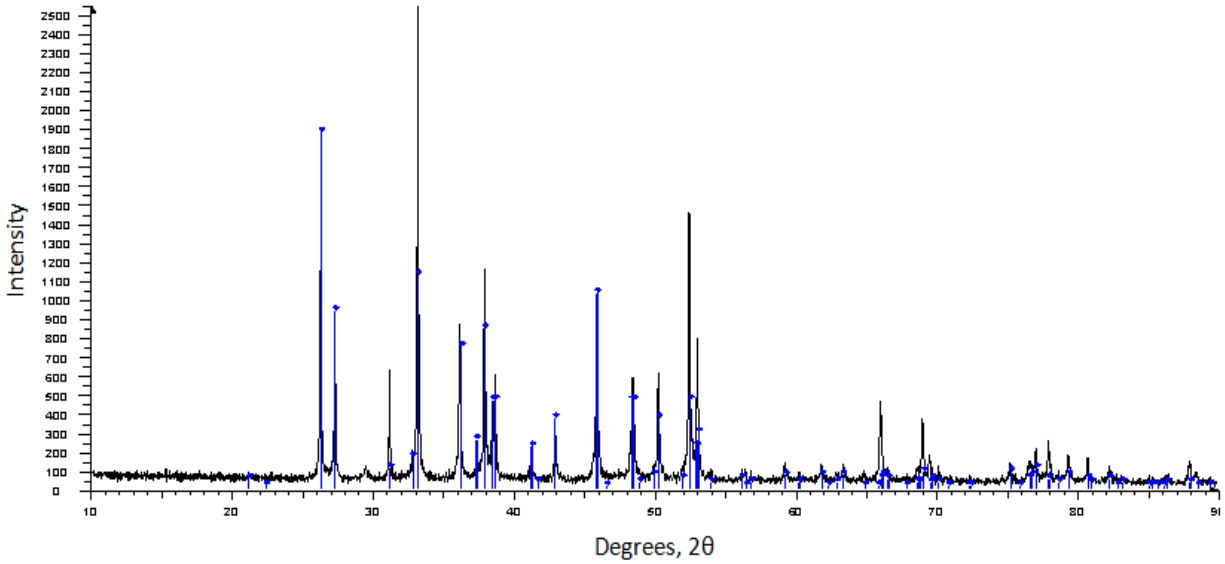

Fig. 6 *X-Ray Diffractogram of mussel powder*

3.2 Scanning Electron Microscope (SEM)

SEM images of the previous fractured tensile specimen for neat epoxy resin and toughened epoxy with mussel shell powder (TEMP) at 500x magnification are shown in Fig. 7. Fig. 7(a) demonstrates that the cracked neat epoxy resin surface was smooth and cleaved, signifying a brittle fracture. It also showed less continuous fracture patterns compared to other TEMP fractions. At the 2.5% TEMP, the mussel shell particle was seen and well bonded with the epoxy matrix, as illustrated in Fig. 7(b), with no voids observed at the mussel shell particles/epoxy interface. The addition of mussel shell particles enhances the roughness of fracture surfaces. It is shown that the mussel shell particle and epoxy matrix are compatible and allow for effective stress transmission from matrix to particles. Crack deflectors and crack pinning were also seen by the incorporation of mussel shell particles.

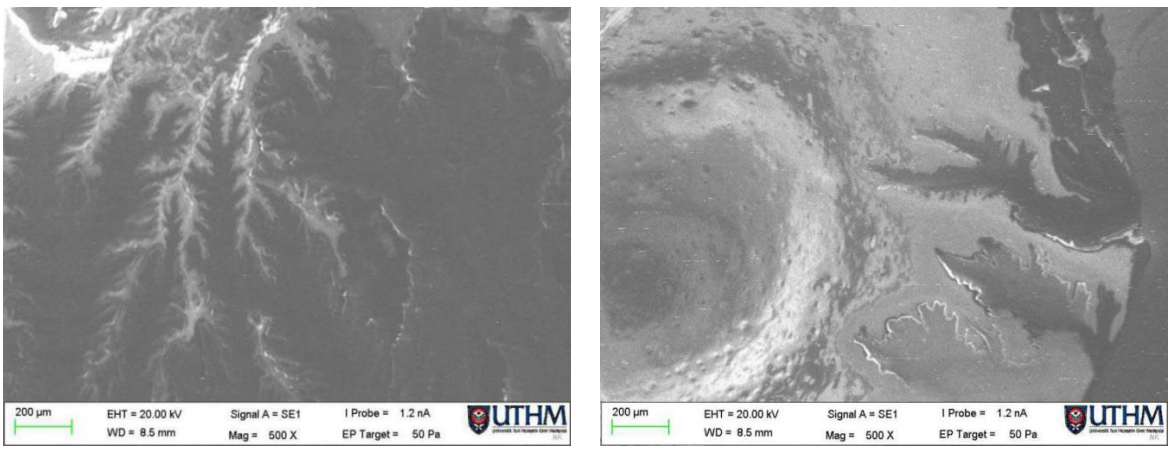

(a) **(b)**

Int. Journal of Integrated Engineering Vol. 16 No. 1 (2024) p. 201-212

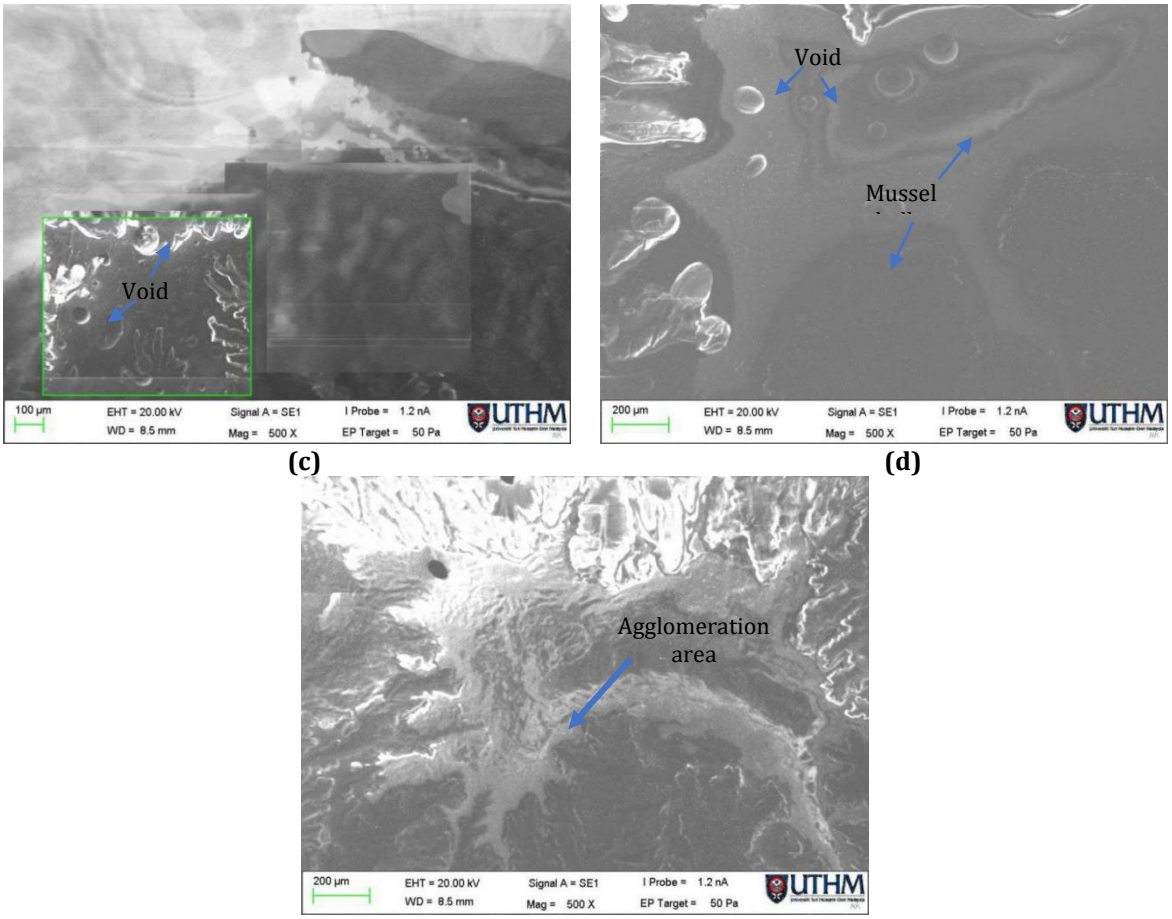

Fig. 7 *SEM photographs with respective to different mussel powder volume fractions (a) 0%; (b) 2.5%; (c)5%; (d)7.5%; (e) 10%*

Fig. 7(c) and Fig. 7(d) show the micro-graphs of the fractured surfaces of 5% and 7.5% of TEMP. The TEMP looks as unevenly coarse and rough with an affected fracture path, which is attributed to the inclusion of filler. Both TEMP samples had a greater degree of roughness, while they showed better adhesive bonding between the epoxy resin and the mussel shell particles. The SEM analysis of 2.5%, 5% and 7.5% TEMP showed that the mussel shell powder particle and matrix have excellent wettability. Moreover, void content increased as the volume fraction of TEMP grew from 2.5 to 10%. Although degassing had been performed before molding, voids were still seen, inducing crack blunting. The void contents significantly affected the mechanical properties and performance of TEMP [18].

Fig. 7(e) also shows a fractured sample of 10% mussel shell powder, demonstrating poor adhesion to the epoxy matrix. The fracture surface becomes amorphous once the mussel shell powder is added. Furthermore, the polymer matrix generates stress concentration zones, which causes early failure. The arrangement of mussel shell particles shows that they are not well bonded with the epoxy matrix, which is called agglomeration. Agglomeration is a sign of insufficient matrix filler dispersion. These agglomerates are stress concentration zones that facilitate fracture initiation and propagation, leading to brittle failure. Porosity flaws in the epoxy mixture containing a 10% volume fraction of mussel shell powder are predicted to reduce the joint strength and fracture energy value. This porosity defect is induced by the stirring and weak degassing processes, which trap air in the epoxy mixture containing mussel shell powder [19]. As seen in Fig. 7(e), porosity makes the connection brittle because trapped air generates an empty void.

3.3 Load-Displacement Profile of SLJ

Fig. 8 shows the load variation according to the displacement of a single lap joint tensile test. Initially, load-displacement curves are linear, and the capacity abruptly decreases upon reaching maximum loading. The ultimate tensile loading point serves as the critical load at failure. The critical fracture load was dependent upon the strong viscosity properties of the TEMP. The crack begins as cohesive fracture reaches the ultimate load, and then cracks propagate rapidly, decreasing loading resistance. Fig. 8(a) shows an elastic zone followed by a complete fracture of the sample, demonstrating brittle failure. Point (i) represents the initiation of damage. This

event is associated with micro-damage, such as matrix cracking and fiber bridging. Point (ii) occurred as the adhesive fracture reached process zone length. In cohesive failure mode, the adhesive failure occurred within the adhesive layer. This suggests that Point (ii) occurred in a short period of time, and the complete separation occurred at Point (iii), as seen in Fig. 8(a). Incorporating a mussel shell as a filler enhances tensile strength, as shown in Fig. 8(b). The highest stiffness was obtained at the 7.5% mussel shell volume fraction. As discussed previously, increasing mussel shell concentration is prone to particle agglomeration and stress concentration.

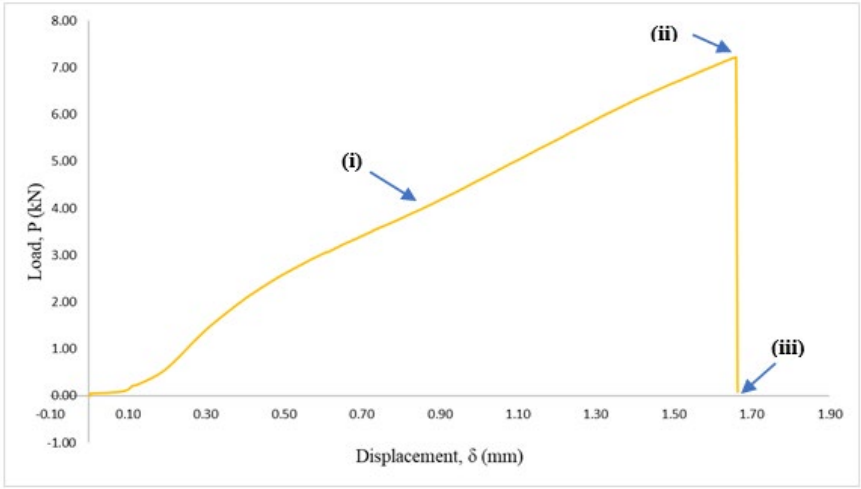

(a)

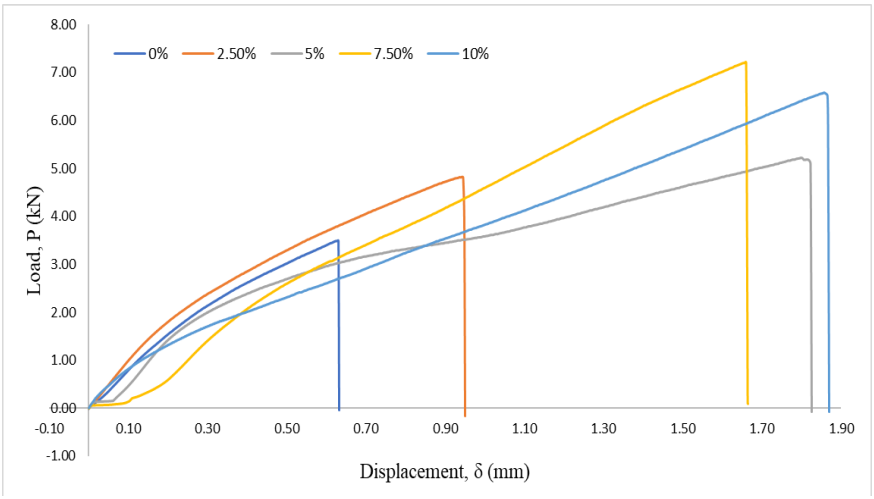

(b)

Fig. 8 *Load-displacement profiles (a) the typical load-displacement profile (taken from SLJ-7.5%-12.7mm overlap length);the load-displacement profiles respective to mussel powder fraction in 12.7mm overlap length*

3.4 Failure Modes

The mechanical characteristics of the adhesive and adherends affect the failure modes of a joint [20]. According to the experimental findings, all TEMP adhesively bonded single-lap joints indicate cohesive failure modes, in which the adhesive is still attached at both surfaces of the adherends. Cohesive failure occurs in the TEMP adhesively bonded single-lap joint due to a massive crack that entirely crosses the epoxy bond line and leaves two split epoxy sections on both fracture surfaces, as shown in Fig. 9. Moreover, cohesive failure occurs, indicating that cohesive forces within the adhesive are weaker than the interfacial bonding between adhesive and steel adherend. The fracture initiation was invisible due to the microcrack, which is difficult to observe.

3.5 Shear Strength of Single Lap Joint

Table 2 shows the strength of SLJs at various mussel shell powders and overlap length. According to Table 2, the ultimate load at failure increased with the increased overlap length for all mussel shell content. The joint strength varies between 3.24 to 11.91 kN. At the overlap length of 12.7 mm, the ultimate load at failure, Pmax improved from 3.24 kN of neat epoxy resin to 4.56 kN, 4.97 kN and 6.603 kN with the incorporation of 2.5%, 5% and 7.5%

Int. Journal of Integrated Engineering Vol. 16 No. 1 (2024) p. 201-212

mussel shell volume fraction, respectively. For all overlap lengths, the shear strength of single-lap joints tended to increase up to a volume fraction of 7.5% before showing a declining trend. The addition of 10% mussel shell powder, the adhesives become less workable, decreasing wettability with the surface of the adherend. The optimum joint strength was attained at 7.5% mussel shell powder with strength enhancement in the range of 103.7% to 169.6% for the overlap length studied compared to neat epoxy. The improvement is much higher than those reported Anac and Dogan [12] when they studied the joint strength improvement of epoxy adhesive filled with mussel shell, olive pomace, and walnut powder. They reported that the improvement was maximum 26% compared to neat epoxy at the same overlap area. Yip et al. [13] reported an improvement in joint strength by a maximum of 25% using epoxy adhesive filled with 5% eggshell powder.

Fig. 9 *Cohesive failure modes seen upon testing (taken from SLJ-5%-25.4mm overlap length)*

Table 2. *Shear strength of SLJ specimen tested*

Volume fraction of mussel powder (%)	Overlap length (mm)	Series Designations	Mean ultimate load at failure, P_{max} (kN)	Joint strength enhancement (%)*	Failure modes
0	12.7	SLJ-0-12.7	3.242 ± 0.224	-	cohesive
	25.4	SLJ-0-25.4	4.226 ± 0.415	-	cohesive
	38.1	SLJ-0-38.1	4.295 ± 0.069	-	cohesive
	50.8	SLJ-0-50.8	5.120 ± 0.623	-	Cohesive
2.5	12.7	SLJ-2.5-12.7	4.564 ± 0.367	40.8	cohesive
	25.4	SLJ-2.5-25.4	6.745 ± 0.316	60.0	cohesive
	38.1	SLJ-2.5-38.1	6.949 ± 1.042	61.8	cohesive
	50.8	SLJ-2.5-50.8	8.567 ± 2.839	67.3	cohesive
5	12.7	SLJ-5-12.7	4.969 ± 0.420	53.3	cohesive
	25.4	SLJ-5-25.4	6.871 ± 0.196	62.6	cohesive
	38.1	SLJ-5-38.1	8.175 ± 0.549	90.3	cohesive
	50.8	SLJ-5-50.8	8.711 ± 0.119	70.1	cohesive
7.5	12.7	SLJ-7.5-12.7	6.603 ± 0.534	103.7	cohesive
	25.4	SLJ-7.5-25.4	8.242 ± 2.544	95.0	cohesive
	38.1	SLJ-7.5-38.1	11.580 ± 0.761	169.6	cohesive
	50.8	SLJ-7.5-50.8	11.910 ± 3.337	132.6	cohesive
10	12.7	SLJ-10-12.7	6.217 ± 0.327	91.8	cohesive
	25.4	SLJ-10-25.4	8.760 ± 1.603	107.3	cohesive
	38.1	SLJ-10-38.1	11.105 ± 2.074	158.6	cohesive
	50.8	SLJ-10-50.8	8.741 ± 2.449	70.7	Cohesive

*The baseline is neat epoxy at the corresponding overlap length

If compared to that of 7.5% mussel shell content, the shear strength of 10% mussel shell decreases, possibly due to particle agglomeration. The agglomeration of mussel shell powder decreases the particles surface area, which leads to stress raisers since the particles clump together and act as micro-particles [21]. Agglomeration also reduces the bonding strength between the particles and the epoxy resin. Additionally, particle aggregation acts as a concentrated stress zone when the cohesiveness between the particles is inadequate. According to Sugiman et

al. [2], the fracture surfaces become smoother as the fly ash volume fraction rises. This suggests that adding more fillers to the epoxy causes it to become more brittle.

In general, the joint strength increases with the increase of overlap length up to a certain overlap length and then to be constant, as shown in Fig. 10. The ultimate strength of 5% TEMP bonded single-lap joints rises as the adhesive overlap length increases, as shown in Table 2. Moreover, the longer overlap length, which is 50.8 mm, provides a larger bonding surface, and promotes stronger joints, as expected. Raos et al. [22] found the maximum strength at the overlap length of 40 mm. This optimal overlap length leads to optimal overall joint strength. But the optimal overlap length may be different with the different types of adhesives. The longer overlap length beyond this optimal value leads the joint's load bearing to deteriorate, and adherend extends into the plastic area. Moreover, voids play the main role, as the longer overlap length contains more voids which induces plastic deformation at the end of overlap and leading to premature failure. At a higher volume fraction exceeding 10%, the adhesives are prone to being more viscous and are unable to wet the adherend surface easily. It is noticed from Fig. 11 that the shear strength increased to 6.949 kN, 8.175 kN, and 11.58 kN with the incorporation of 2.5%, 5%, and 7.5% mussel volume fractions. Additionally, the stress distribution will be more equally distributed throughout the lap joint. In this case, the optimal value may be achieved by modifying the overlap length of each adhesive. Here, the tension stress within the adherends and the strength of the adhesive joint has reached equilibrium.

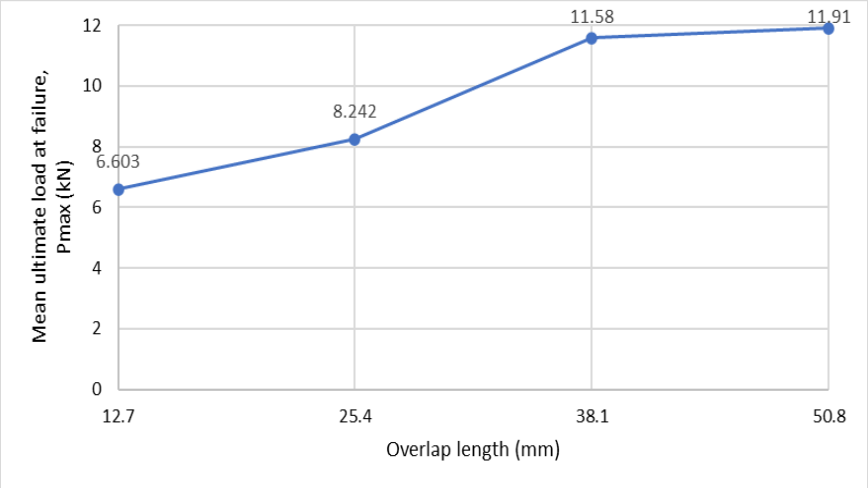

Fig. 10 *Shear strength as a function of overlap length (taken from SLJ-7.5%)*

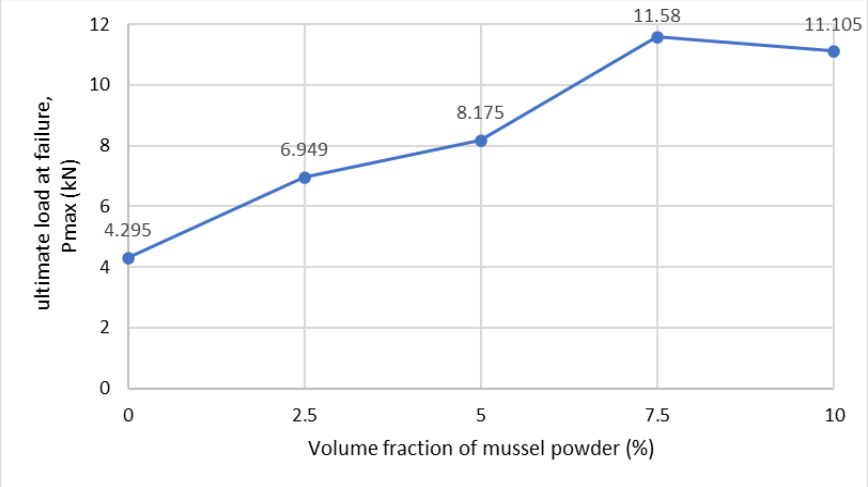

Fig. 11 *Shear strength as a function of mussel shell powder addition (taken from SLJ-38.1mm overlap length)*

4. Conclusion

A series of toughened epoxy with mussel shell powder (TEMP) was developed based on mussel shell powder and Epikote 828 epoxy resin. From the physical testing, mussel powder has substantial calcium carbonate content and is suitable for use as fillers in epoxy resin. Filler volume fractions and overlap length significantly influenced the

ultimate load of the single lap joint. The optimum joint strength is attained at the 7.5% mussel shell powder with the strength enhancement in the range of 103.7% - 169.6% for the overlap length studied (12.7 - 50.8 mm). On the contrary, ultimate strength declines at 10% TEMP due to particle agglomerations. A combination of an overlap length of 50.8 mm and 7.5% TEMP gives optimal ultimate load failure at 11.91 kN compared to other testing series. All test specimens demonstrated cohesive failures, which indicate good bonding between the adhesive developed and the steel adherend. In the research, the mussel shell has not been surface treated and is only considered an adhesive thickness. The joint strength may still be increased by surface treatment of mussel shell and using an optimum adhesive thikness. In future, investigation may also include long-term applications of adhesively bonded structures using the developed adhesives.

Acknowledgement

This research was supported by Universiti Tun Hussein Onn Malaysia (UTHM) through Tier 1 (Vot. Q475) and GGPS (Vot. Q285).

Conflict of Interest

Authors declare that there is no conflict of interests regarding the publication of the paper.

Author Contribution

The authors confirm contribution to the paper as follows: ***study conception and design:*** *Hilton Ahmad, Subashini Velayutham;* ***data collection:*** *Subashini Velayutham;* ***analysis and interpretation of results:*** *Sugiman Sugiman, Hilton Ahmad, Zainorizuan Mohd Jaini;* ***draft manuscript preparation:*** *Sugiman Sugiman, Hilton Ahmad. All authors reviewed the results and approved the final version of the manuscript.*

References

[1] Lu, S. J., Yang, T., Xiao, X., Zhu, X. Y., Wang, J., Zang, P. Y. & Liu, J. A. (2022). Mechanical properties of the epoxy resin composites modified by nanofiller under different aging conditions. Journal of Nanomaterials, 2022, 1–14. https://doi.org/10.1155/2022/6358713

[2] Sugiman, Edy, S., Catur, A. D. & Salman, S. (2018). Effect of fly ash volume fraction on the shear strength of adhesively bonded steel joints. AIP Conference Proceedings, 1983(1), 1-6. https://doi.org/10.1063/1.5046279

[3] Kamath, S. & Ravi Kumar Chandrappa (2021). The Egg shell as a filler in composite materials. Journal of Mechanical and Energy Engineering, 4(4),335-340. https;//doi.org/10.30464/jmee.2020.4.4.335

[4] Barbosa, C., Raul D.S.G. Campilho, Silva, F. & Moreira, R. D. F. (2018). Comparison of different adhesively-bonded joint types for mechanical structures. Applied Adhesion Science, 6(15), 1-19. https//doi.org/10.1186/s40563-018-0116-1

[5] Sandu, M., Sandu, A. & Dan Mihai Constantinescu (2010). Strength of adhesively bonded single-strapped joints loaded in tension. Proceedings of Romanian Academy, 11(4), 371-379.

[6] Campbell, F. C. (2016). Adhesive Bonding and Integrally Cocured Structure. Manufacturing Technology for Aerospace Structure Materials, https;//doi.org/10.1016/B978-185617495-4/50008-1

[7] Redmann, A., Damodaran, V., Tischer, F., Prabhakar, P. & Osswald, T. A. (2021). Evaluation of single-lap and block shear test methods in adhesively bonded composite joints. Journal of Composites Science, 5(27), 1-27. https;//doi.org/10.3390/jcs5010027

[8] Budzik, M. K., Wolfahrt, M., Reis, P., Kozłowski, M., Sena-Cruz, J., Papadakis, L., Nasr Saleh, M., Machalicka, K. V., Teixeira de Freitas, S. & Vassilopoulos, A. P. (2021). Testing mechanical performance of adhesively bonded composite joints in engineering applications: An overview. The Journal of Adhesion, 98(14), 2133-2209. https;//doi.org/10.1080/00218464.2021.1953479

[9] Joao, R.C.C. (2013). Adhesively Bonded Functionally Graded Joints. PhD Thesis, Loughborough University.

[10] Gigante, V., Cinelli, P., Maria Cristina Righetti. & Lazzeri, A. (2020). Evaluation of mussel shells powder as reinforcement for PLA-based biocomposites. International Journal of Molecular Sciences, 21(15), 5364. https;//doi.org/10.3390/ijms21155364

[11] Delzendehrooy, F., Ayatollahi, M. R. & Akhavan, S. A. (2020). Strength improvement of adhesively bonded single lap joints with date palm fibers: Effect of type, size, treatment method and density of fibers. Composites Part B: Engineering, 188, 107874. https://doi.org/10.1016/j.compositesb.2020.107874

[12] Anaç, N. & Do gan, Z. (2023). The effect of organic fillers on the mechanical strength of the joint in the adhesive bonding. Processes, 11, 406. https://doi.org/10.3390/ pr11020406

[13] Yip, C. L., Sugiman, S., Chin, D. & Ahmad, H. (2024). Experimental and numerical investigation of adhesively bonded kfrp/steel double strap joints incorporating eggshell powder-toughened epoxy adhesive. Case Studies in Construction Materials, 20, e02790. https://doi.org/10.1016/j.cscm.2023.e02790

[14] Balda, A (2004). Adhesively-bonded joints and repairs in metallic alloys, polymers and composite materials: Adhesives, adhesion theories and surface pretreatment. Journal of Material Science, 39(1), 1-49. https;//doi.org/10.1023/B:JMSC.0000007726.58758.e4
[15] Loeffen, A., Cree, D., Sabzevari, M. & Wilson, L. D. (2021). Effect of graphene oxide as a reinforcement in a bio-epoxy composite. Journal of Composite Science, 5(3), 1-21. https;//doi.org/10.3390/jcs5030091
[16] Karachalios, E. F., Adams, R. & da Silva, L..F.M. (2013). Strength of single lap joints with artificial defects. International Journal of Adhesion and Adhesives, 45, 69-76.
[17] Macha, I. J., Ozyegin, L. S., Chou, J. & Besim Ben-Nissan. (2013). An alternative synthesis method for Di Calcium Phosphate (Monetite) powders from Mediterranean mussel (Mytilus galloprovincialis) shells. Journal of Australian Ceramic Society, 49(2), 122-128.
[18] Mehdikhani, M., Gorbatikh, L., Verpoest I. & Stepan Lomov. (2018). Voids in fiber-reinforced polymer composites: A review on their formation, characteristics, and effects on mechanical performance. Journal of composite materials, 53(12), 1579-1669. https;//doi.org/10.1177/0021998318772152
[19] Anders, M., Lo, J. F. & Timotei Centea. (2016). Eliminating volatile-induced surface porosity during resin transfer molding of a benzoxazine/epoxy blend. Composites Part A: Applied Science and Manufacturing, 84, 442-454. https;//doi.org/10.1016/j.compositesa.2016.02.024
[20] Chung, S. H., Park, B. C., Chun, H. J. & Park, J. C. (2017). Experimental study on failure mechanism of single lap-shear bond joint with dissimilar materials. Journal of Physics: Conference Series, 843(1), 012020. https;//doi.org/10.1088/1742-6596/843/1/012020
[21] Zare, Y. (2016). Study of nanoparticles aggregation/agglomeration in polymer particulate nanocomposites by mechanical properties. Composites Part A: Applied Science and Manufacturing, 84, 158–164.
[22] Raos, P., Kozak, D. & Lucic, M. (2007). Stress-strain analysis of single-lap tensile loaded adhesive joints. AIP Conference Proceedings, 908, 1093–1098.